Fig. 5 $\Delta a = a - a_0$, $\alpha = \mu = 0$, $\gamma = 150$. Computations show that when $\gamma \neq 0$, the displacement of the circular axis may have an oscillatory character.

When $\beta = \gamma = 0$, Eq. (13) may be written as a law of conservation of energy and momentum:

$$\sqrt{\Lambda_R}\, aR^2\dot{R} = \pm\sqrt{(a_0 - aR^2)(aR^2 - a_0R_\Delta^2) + \frac{a_0\delta}{\varkappa - 1}\left[aR^2 - a_0^{\varkappa-1}(aR^2)^{2-\varkappa}\right]},$$

$$aR^2\dot{a} = \mu a_0,\ aR^2\dot{Z} = \alpha a_0, \tag{14}$$

where $R_\Delta = \sqrt{(\alpha^2 + \mu^2)/2}$. The signs + and − in front of the radical correspond to expansion and collapse of the bubble. The last two equations (14) lead to an explicit relation $Z = \alpha(a - a_0)/\mu$ which makes it possible to eliminate the equation for Z from further analysis. Equating the expression within the radical to zero, we obtain a relation between the parameters of the problem when the bubble radius has extremal values.

In the case of the collapse of the bubble ($\delta = 0$, $R < 1$) the first two equations of the system (14) describe the motion of the bubble between the states a_0 and $a_0R_\Delta^2$. If $\mu > 0$, $R_\Delta > 1$ then $a_0 \leqslant aR^2 \leqslant a_0R_\Delta^2$; if $\mu < 0$, $R_\Delta < 1$ then $a_0R_\Delta^2 \leqslant aR^2 \leqslant a_0$. When minimum radius R_Δ is attained, the bubble size and speed are determined from

$$\dot{a}\Big|_{R=R_\Delta} = \frac{\mu}{R_\Delta^2},\ \dot{Z}\Big|_{R=R_\Delta} = \frac{\alpha}{R_\Delta^2}.$$

Computed results for the system (13) in the case of the collapse of the empty bubble are given in Fig. 6 where $\alpha = \beta = \gamma = \delta = \varepsilon = 0$, $a_0 = 10^4$ and lines 1-5 correspond to $\mu = 1.25, -1, -0.75, -0.5$, and -0.25.

LITERATURE CITED

1. V. K. Kedrinskii, "One dimensional pulsation of toroidal gas bubble in compressible fluid Zh. Prikl. Mekh. Tekh. Fiz., No. 3 (1977).
2. E. Yanke, F. Emde, and F. Lesh, Special Functions [in Russian], Nauka, Moscow (1964).
3. A. T. Onufriev, "Theory of vortex ring motion under the action of gravity. The ascent of the mushroom cloud from atom explosion," Zh. Prikl. Mekh. Tekh. Fiz., No. 2 (1967).
4. G. Lamb, Hydrodynamics, Dover, New York (1945).
5. L. E. Frenkel, "Examples of steady vortex rings of small cross section in an ideal fluid," J. Fluid Mech., 51, No. 1 (1972).

INVESTIGATION OF HEAT TRANSFER IN SEPARATED REGIONS IN A SUPERSONIC LAVAL NOZZLE

E. G. Zaulichnyi and V. M. Trofimov

UDC 536.24:532.54

1. This paper describes experiments and an approximate method to compute heat transfer at the wall in supersonic flow with separation in the presence of a step-cavity profile of the divergent part of the Laval nozzle. Tests were conducted on a horizontal jet facility in which a plane nozzle with cavities (Fig. 1a) was mounted. Local heat transfer and pressure coefficients at the nozzle walls, including the separate region, were measured. Special thin film gauges [1] were used to measure heat transfer coefficients under complex flow conditions. The flow parameters were as follows: stagnation temperature $T_0 = 250$-$270°K$, total pressure $p_0 = (9.0\text{-}12.5)\cdot 10^5$ Pa, and Reynolds number based on the throat section dimension, $Re = 6\cdot 10^6$. Measurements were made on three models of the nozzle with Mach numbers at the separation point at the edge of the cavity: 1.90, 2.28, and 2.61, respectively. A schematic diagram of the cavity is shown in Fig. 1a. The length of the horizontal wall of the cavity had the following values: L = 0, 14, 27, 47, and 60 mm. The height of the wall h = 12 mm was kept constant in all the tests and was appreciably more than the boundary layer thickness ahead of separation ($\delta_1/h = 0.13$-0.17).

Novosibirsk. Translated from Zhurnal Prikladnoi Mekhaniki i Tekhnicheskoi Fiziki, No. 1, pp. 99-106, January-February, 1986. Original article submitted September 7, 1984.

0021-8944/86/2701-0088$12.50

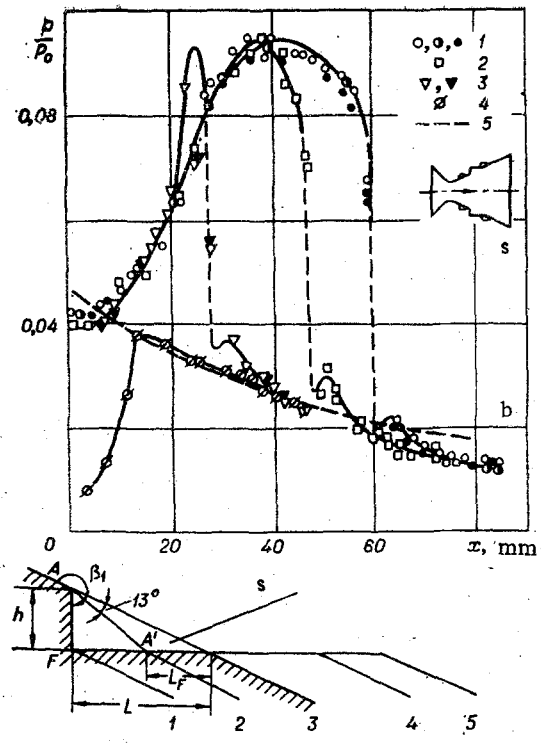

Fig. 1

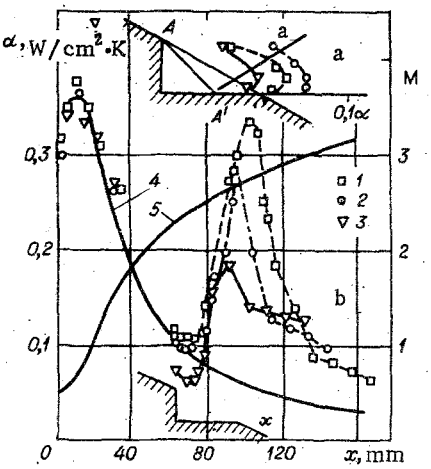

Fig. 2

Let us determine the basic types of cavities in the nozzle contour as a function of its horizontal length. The cavity obtained by the removal of a part of the nozzle contour is called the cavity without the displacement of the nozzle contour. If the length of the horizontal wall of the cavity is increased by protruding a part of the nozzle into the flow, then it results in a cavity with a positive displacement of the nozzle contour; if, however, the same wall is shortened by moving the part of the nozzle contour in the opposite direction, then a cavity with negative nozzle contour displacement is obtained. In the present tests, conditions without displacement corresponded to a cavity with the length of the horizontal wall L = 27 mm, condition with positive displacement was achieved with L = 47 and 60 mm, and for negative displacement L = 14 mm. The shape of the cavity of different types is shown schematically in Fig. 1 below (1-5).

Pressure measurements at the nozzle walls and the cavity showed that pressure decreases sharply behind the separation point, remains constant over a certain region and then increases, reaching high values in the region behind the shock (s) whose dimensions depend on the length of the cavity. This region corresponds to the reattachment location of the separated flow. It is also worth noting that under all flow conditions and for all types of cavities the pressure along the nozzle contour behind the cavity is above the design value for the flow in the nozzle without the cavity. Pressure distributions for different types of cavities are shown in Fig. 1b with Mach number at the point of separation $M_1 = 2.61$. Here p/p_0 is the ratio of the static pressure at the wall to the total pressure. It is seen that for cavities without displacement of the nozzle contour (point 3) and with positive displacements (points 1 and 2), the maximum pressure at reattachment is identical. Here the width of the high pressure regions increases with increase in the cavity length. For cavities with negative displacement (point 4) no appreciable increase in pressure at reattachment is observed. Curve 5 is the designed pressure for the nozzle without cavity. Our test data for pressures behind reattachment shock with positive displacement of the contour are well approximated by the relation

$$\frac{p_w}{p_b} = \left(0.6 + 4.4x_F - 2.94x_F^2\right)\frac{M_1}{2.28}, \qquad (1.1)$$

where x_F is the coordinate along the horizontal cavity wall from the point A' downstream (see Fig. 1b) divided by the length of the segment from the point A to the end of the cavity; p_w is the wall pressure from the point A downstream; p_b is the base pressure on the vertical wall of the cavity AF and in the region FA' of the horizontal wall (experimental dependence of p_b on the turning angle of the flow at the point A and M_1 is given in [2]). Equation (1.1) is a good approximation for the experimental results in the range $0.2 \leqslant x_F \leqslant 1.0$. In the range

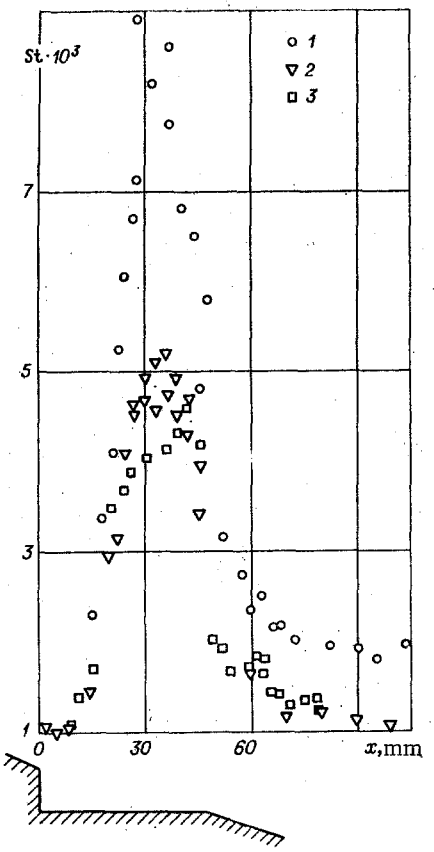

Fig. 3

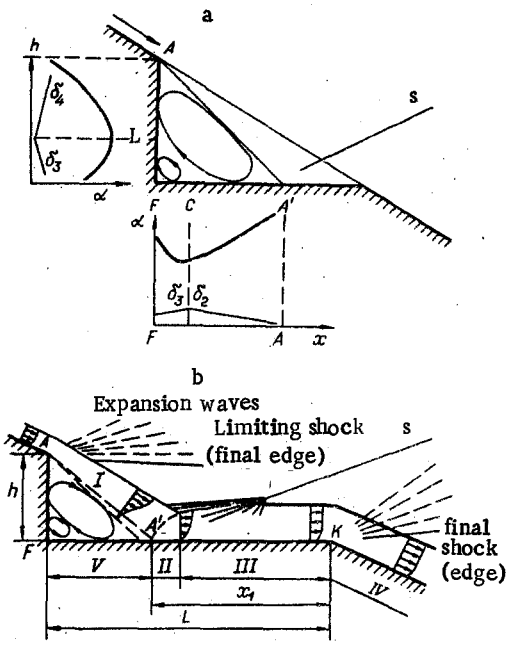

Fig. 4

$0 \leqslant x_F \leqslant 0.2$, test points are described by a straight line between the ordinates at $x_F = 0$ and 0.2. The location of the point A' (see Fig. 1b) is determined by the turning angle of the flow in the expansion behind the separation at the point A. In all the tests for cavities with positive displacement and without displacement, this angle was maintained constant and equal to $\sim 13°$ independent of the Mach number at separation.

The agreement between heat-transfer coefficients and the pressure distribution along the walls of the cavity in the nozzle was observed in [3]. Furthermore, it was mentioned that the heat transfer in the nozzle contour behind the cavity remained, unlike the pressure, considerably higher than the design values obtained for flows in the nozzle without cavity. Test results are shown in Fig. 2 for the local heat-transfer coefficients for different cavities. For the flow condition with $M_1 = 2.28$ points 1-3 correspond to L = 47, 27, and 14 mm. Curve 4 is for the computed data from [4] for the flow in the nozzle without cavity, 5 is the Mach number distribution along the nozzle. Just as in the case of the pressure distribution, with a decrease in the horizontal length of the cavity but for a given height, a peak in the heat flux (in the reattachment zone) is observed in the narrower region. Its maximum lies in the neighborhood of the pressure maximum though displaced a little downstream.

A comparison of experimental data for cavities with fixed positive displacement at different locations of the nozzle shows a significant effect of streamwise velocity gradient of the mean flow on heat transfer. Figure 3 shows the distribution of Stanton number $St = \alpha/(c_p \rho u)$ (α is the local heat-transfer coefficient, c_p is the specific heat at constant pressure, ρ and u are the density and velocity of the flow for three different sections of the nozzle). In order to eliminate interaction of separated zones, measurements were made on individual cavities on three nozzle models. Points 1-3 (Fig. 3) correspond to cavities of length L = 47 mm at nozzle sections with Mach numbers at separation at the edge of the cavity $M_1 = 1.90$, 2.28, and 2.61. It is seen that with an increase in velocity gradient of the mean flow in the nozzle there is an increase in heat transfer at the walls of the separated region. The maximum value of the streamwise velocity gradient is attained, as is well known, in the transonic region of the flow. The distribution of Stanton numbers along the cavity located in the neighborhood of this region (Fig. 3, point 1) indicates significant increase in heat transfer relative to cavities downstream (points 2 and 3). On the other hand, in sections

with less intense variation in streamwise velocity gradient, the difference in heat-transfer distribution in separated regions is insignificant (Fig. 3, points 2 and 3). The same trends are observed for cavities without displacement. For cavities with negative displacement the effect of the mean streamwise velocity gradient on heat transfer was not observed.

Heat transfer on the vertical wall of the cavity and part of the horizontal wall is determined by the peculiarities of reverse flow. Experimental distribution of heat-transfer coefficients on the vertical wall of the cavity (see Fig. 2a) indicates the presence of a small maximum. The nature of such a variation in heat transfer on the vertical wall of the cavity as also the minimum on the horizontal wall in the separated recirculation zone is explained by the presence of two vortices (Fig. 4a). The flow in the near-wall region of the recirculation zone can be considered from the point of view of a boundary-layer model. In this case the boundary layer δ_2 develops from the point A'. The second vortex forms the opposite boundary layer δ_3. The point C lies at the section where the thickness of these layers is a maximum which is characterized by the minimum of heat flux on the horizontal wall of the cavity. The point L on the vertical wall is the frontal, i.e., the confluence point of two vortices. Boundary layers δ_3 and δ_4 develop from this point. Hence the point L is characterized by maximum heat flux on this wall of the cavity.

Measurements of heat fluxes on walls in the recirculation zone of the cavity make it possible to determine vortex dimensions. As shown by measurements, the flow stagnates at L and a local increase in pressure is observed in its neighborhood when compared to a constant base in the recirculation zone. These data make it possible to determine recirculation velocity, at least of the primary vortex, interacting with mixing shear layers after separation at the point A.

2. On the basis of studies conducted on the pressure distribution, variation in heat fluxes, and also on flow visualization data [5] in the cavity region, it is possible to suggest a schematic flow model of the boundary-layer type with complex wave structure of the external region (see Fig. 4b).

At the point A', whose location depends on reattachment conditions, an increase in pressure is initiated. It is "shot" into by the resultant shock due to compression waves in which a contraction of the mixing jet takes place during its interaction with the cavity wall or with the extension of the nozzle contour depending on the type of the cavity. The shear layer at the interaction region with the wall is strongly turbulated [6-9]. This interaction causes an increase in the turbulence level not only in the compression region but also in the recirculation zone and beyond the compression region.

Depending on the flow conditions, the computational domain for the heat-transfer distribution is divided into the following parts (see Fig. 4b): I is the flow past the edge of the step from the separation point A to the beginning of the pressure increase A', into which the oblique attached shock is "shot" (region of the free shear layer); II is the interaction region of the shear layer with the wall of length of the order of the shear layer thickness ahead of the point A' in which a new boundary layer is formed with the appearance of new boundary conditions for the flow on to the wall; III is the region where the new boundary layer grows under the conditions of compression and higher turbulence level caused by the interaction of the flow with the wall; IV is the region behind the compression zone (behind the point K) where the increased turbulence level relaxes to the turbulence level in the undisturbed flow; V is the reverse flow region.

In order to compute heat transfer at the reattachment point A' (see Fig. 4b) the characteristic parameters are the thickness of the shear layer at the point A' and the angle at which the shear layer begins to reattach. The effective origin of the formation of the shear layer is found from the condition for the equality of the energy thickness of the shear layer at the separation point and the energy thickness of the thermal boundary layer on the nozzle wall at the same point. The latter is computed on the basis of the limiting laws for skin friction and heat transfer [4] under the conditions of compressible flows, nonisothermal conditions, and the presence of streamwise pressure gradient. Apart from the inclusion of the factor of succession for the computation of the shear layer at the point A', it is necessary to know the rate of the increase or the expansion parameter of the shear layer which is determined, e.g., according to [8]. The influence of the interaction angle of the shear layer with the cavity wall at the reattachment location could be taken into account in the first approximation by multiplying the energy thickness by the cosine of this angle. Such an operation for the zero reattachment angle leads to the conservation of energy thickness of the

shear layer and for an angle of 90° the point A' becomes base. In what follows the computation of heat transfer at the point A' is carried out within the framework of the same theory [4].

The boundary-layer approximation is not valid in region II, but since it is short for relatively thin preseparation boundary layers, the computation can be extended from the beginning of region III, assuming the point A' to be the effective origin for the new boundary layer. The assumption of the appearance of a new boundary layer at the reattachment location of the separated flow is justified by the sharp variation of the lower boundary condition for the shear layer, causing an almost instantaneous rearrangement of the structure of the wall layer. Similar considerations were used, i.e., in [10] for the computation of heat transfer in the case of subsonic flows in a channel. Thus, a thermal boundary layer is developed, starting from the point A' with $dp/dx \neq 0$ and variable temperature along the wall. In order to carry out one-dimensional computation of the flow outside the boundary layer on the nozzle walls, the plane nozzle in the present case is replaced by an axisymmetric nozzle whose area at each cross section is equivalent to the plane nozzle. The horizontal wall of the cavity becomes a cylindrical surface and the computation is carried out using the general method [4] for the flow in an axisymmetric nozzle. The flow in the external boundary layer has a wavy character due to the strong influence of the compression shock (see Fig. 4b). The shock angle is determined on the basis of the computed Mach number ahead of the shock and the measured pressure rise in the shock. The flow parameters at the outer edge of the boundary layer (e.g., Mach number) during the transition through the fan of compression waves, corresponding to the shock, do not change instantaneously. Hence, in order to make precise computation of the Mach number, an interpolation with a quadratic polynomial was used in the region from the point A' to the location of maximum pressure behind the shock ($x_F = 0.75$). In order to determine ρu at the outer edge of the boundary layer in region III, besides Mach number, it is also necessary to know the pressure distribution along the cavity wall (1.1). In region IV ρu is determined from the known discharge and nozzle geometry. In the neighborhood of the point K at the boundary of regions III and IV the curves for ρu are combined using the method of mean squares.

3. The computation of heat transfer showed (Fig. 5, curve 1) that in region III there is a significant disagreement with the experiment. As mentioned above, in region III the flow has a higher turbulence level and its influence on skin friction has a stable character [6]. The increase in heat transfer and skin friction in this case is up to 80% and more [6, 1]. The effect of increased turbulence level in the boundary layer on the heat-transfer coefficient is found from the analogy with the relation for the skin friction coefficient recommended in [6]:

$$\mathrm{St} = \frac{c_{f0}}{2}\,\mathrm{Pr}^{-0,75}\left[1 + 200\,(\varepsilon - \varepsilon_0)^2\right]. \tag{3.1}$$

Here, c_{f0} is the skin coefficient, taking into account various disturbance factors [4] but without the consideration of increased turbulence level; Pr is the Prandtl number; ε is the turbulence level in the flow, determined by the ratio of root-mean square value of the fluctuations $(\rho u)'$ to the mean value ρu; ε_0 is the turbulence level in the undisturbed flow. This relation proved to be very effective for the interaction of vortices with a wall [1] and agrees satisfactorily with results [7] up to $\varepsilon \leqslant 6$-8%.

In region IV the effect of higher turbulence level on heat transfer decreases. There is a mixing of the mean flow having 1% turbulence level with the wall layer in which ε_1 at the origin of region IV is determined from [8]. The intensity and duration of the effect of increased turbulence level on the heat-transfer characteristics in the region IV is recommended to be determined from the fluid flow characteristics in the nozzle [11]. Then the effectiveness of fluid mixing in the nozzle is expressed by the relation

$$\theta = \left[1 + 0,25\left(\frac{D_*}{D_1}\right)^{-1,25} (\mathrm{Re}_*/(\mathrm{Re}_T^{**})^{1,25}) \left(\int_{x_1}^{x} \Psi_t \Psi_M \left(\frac{\mu_w}{\mu_0}\right)^{0,25} \left(\frac{D_*}{D}\right)^{0,75} dx\right)\right]^{-0,8}, \tag{3.2}$$

where μ_0, μ_w are the coefficients of viscosity at temperature T_0 and wall temperature T_w; $\mathrm{Re}_* = 4G/(\pi\mu_0 D_*)$ is the Reynolds number; G is the fluid flow rate in the nozzle; D_* is the throat diameter; $(\mathrm{Re}_T^{**})_1 = \rho u \delta_{T_1}^{**}/\mu_0$ is the Reynolds number based on energy thickness at the section $x = x_1$; x corresponds to the nondimensional coordinate x/D_*; Ψ_t, Ψ_M are coefficients that take into consideration effects of nonisothermal conditions and compressibility; the index 1 denotes here the boundary between regions III and IV.

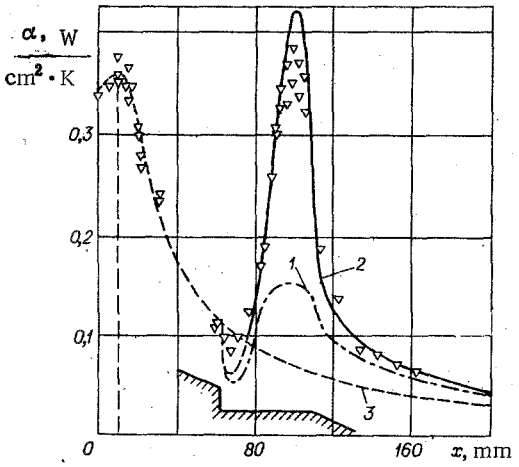

Fig. 5

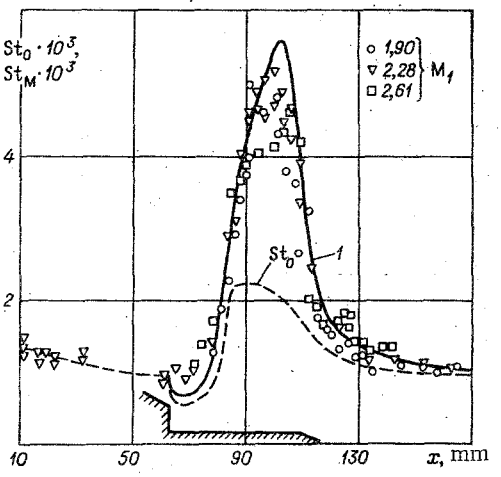

Fig. 6

Increased turbulence level is found from the relation

$$(\varepsilon - \varepsilon_0)^2 = (\varepsilon_1 - \varepsilon_0)^2\theta,$$

where θ is computed from (3.2); $\varepsilon_0 = 0.01$.

A comparison of computed results with experimental data along the entire zone of separation, compression region and downstream of it indicates a satisfactory agreement (Fig. 5, curve 2). Computation based on the same method and model of turbulent boundary layer without an increased turbulence level gives values lower than the experimental results (Fig. 5, curve 1). The curve 3 corresponds to computation without cavity, ∇ are experimental points. Mass transfer was computed in the same way as the heat transfer. Here the increased turbulence level was determined from the same measurements [8].

In view of the above-described dependence of heat transfer on the streamwise velocity gradient, Eq. (3.1) was slightly modified to generalize the data on heat transfer:

$$\mathrm{St} = \mathrm{St}_0\left\{(1 + 200\,(\varepsilon - 0.01)^2)\left[1 + 1.45\left(\frac{d}{d\xi}\left(\frac{1}{u}\frac{du}{d\xi}\right)\right)^2\right]\right\}.$$

Here $\xi = x/D$; x is the coordinate along the undistorted nozzle contour. Such a modification makes it possible to take into consideration the additional effects of streamwise velocity gradient on the increase in heat transfer, which, apparently, is especially manifested in the transonic region, where the normal velocity component is large. The latter, in fact, increases the extent of the interaction of the jet mixing with the cavity wall, thereby increasing the turbulence level.

The generalization of experimental data according to streamwise velocity gradient (and Mach number) at the separation point is shown in Fig. 6, where $\mathrm{St}_M = \mathrm{St}\Big/\left(1 + \left(\frac{d}{d\xi}\left(\frac{1}{u}\frac{du}{d\xi}\right)\right)^2\right)$ is the modified Stanton number, the cavity length L = 47 mm, and height h = 12 mm. The nozzle throat section is given by the coordinate x = 10 mm. It is seen that computation based on the method suggested here (curve 1) satisfactorily agrees with experimental data on the entire contour, including the cavity.

LITERATURE CITED

1. V. N. Zaikovskii, E. G. Zaulichnyi, et al., "Experimental study on local heat-transfer coefficients on the walls of a valve," Zh. Prikl. Mekh. Tekh. Fiz., No. 2 (1982).
2. E. G. Zaulichnyi, Yu. L. Makarevich, and G. B. Trubachev, "Investigation of the characteristic distribution of gasdynamic parameters in supersonic separated flows in Laval nozzle," in: Gasdynamics of Flows in Nozzles and Diffusers [in Russian], Inst. Teor. Prikl. Mekh., Sib. Otd. Akad. Nauk SSSR, Novosibirsk (1982).
3. E. G. Zaulichnyi, Yu. L. Makarevich, B. M. Melamed, et al., "Experimental methods and results of the study on the local heat transfer on the nozzle contour in the separated region," in: III All-Union School on Methods in Aerophysics [in Russian], Vol. 2, Inst. Teor. Prikl. Mekh., Sib. Otd. Akad. Nauk SSSR, Novosibirsk (1982).

4. S. S. Kutateladze and A. I. Leont'ev, Heat and Mass Transfer and Skin Friction in Turbulent Boundary Layer [in Russian], Énergiya, Moscow (1972).
5. G. A. Grigor'ev, E. G. Zaulichnyi, V. Ya. Ivanov, and G. B. Trubachev, "Supersonic flow in variable cross-section channel with separated regions," in: Investigation of Wall Layers of Viscous Fluid [in Russian], Inst. Teor. Prikl. Mekh., Sib. Otd. Akad. Nauk SSSR, Novosibirsk (1979).
6. E. P. Dyban and É. Ya. Épik,"Microstructure of boundary layer and transfer processes in them at high turbulence levels of the outer film," in: Proceedings of XVIII Sibir. Teplofiz. Sem., Part II, Inst. Teplo. Fiz., Sib. Otd. Akad. Nauk SSSR, Novosibirsk (1975).
7. A. Slanciauskas and J. Ziugzda, "Regelmäßige Wirbelstrukturen und Warmeübertragungsprozesses," in: Tagung Transportprozesse in Turbulenten Strömungen, Vortrage-Heft III, Berlin (1979).
8. G. S. Settles, D. R. Williams, et al., "Mixing of free turbulent shear layer in compressible fluid," Raketn. Tekh. Kosmonavt., 20, No. 2 (1982).
9. K. K. Horstman, G. S. Settles, et al., "Mixing free shear layer in compressible turbulent flow," Raketn. Tekh. Kosmonavt., 20, No. 2 (1982).
10. M. G. Ktalkherman, "Investigation of separated flows in channel (structure and heat transfer)," Synopsis of Candidate Thesis, Inst. Teor. Prikl. Mekh., Sib. Otd. Akad. Nauk SSSR, Novosibirsk (1971).
11. É. P. Volchkov, V. P. Lebedev, and A. N. Yadykin, "Heat transfer at off-design conditions in Laval nozzle with fluid certain," in: Heat and Mass Transfer VI, Vol. 1, Part 1, Minsk (1980).

PROPERTIES OF THE INTERACTION OF INTERFERENCE AND DIFFRACTION FLOWS AT SUPERSONIC VELOCITIES

M. D. Brodetskii, A. I. Maksimov, and A. M. Kharitonov

UDC 533:6.011:532.526.5

When supersonic flow takes place past angular configurations at angles of attack and slip, a number of interference and diffraction phenomena are observed. Up to now, adequate theoretical [1-10] and experimental [2, 11-22] studies have been performed only on isolated interference and diffraction flows which take place when there is longitudinal flow past an interior or exterior dihedral angle formed by the intersection of plane surfaces.

However, cases of mixed interaction between interference and diffraction flows, which take place, for example, when there is flow past the regions of adjunction of various elements of aircraft, are often encountered in practice. The known theoretical solutions of analogous problems in the linear formulation [1, 3] do not take account of some properties of the real flow. It is therefore of great interest to conduct experimental investigations of such flows on schematized models.

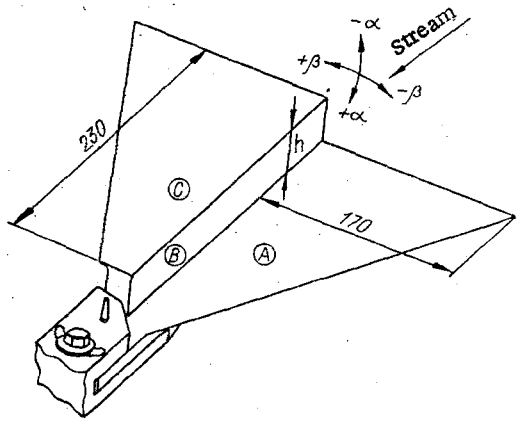

Fig. 1

Novosibirsk. Translated from Zhurnal Prikladnoi Mekhaniki i Tekhnicheskoi Fiziki, No. 1, pp. 106-116, January-February, 1986. Original article submitted October 29, 1984.

 0021-8944/86/2701-0094$12.50